



# May bending radiographs be replaced by recumbent CT scans in patients with adolescent idiopathic scoliosis?

Max Prost<sup>1</sup> · Joachim Windolf<sup>1</sup> · Markus Rafael Konieczny<sup>1</sup>

Received: 9 March 2021 / Revised: 4 July 2021 / Accepted: 22 July 2021 / Published online: 31 July 2021  
© The Author(s) 2021

## Abstract

**Purpose** There is no data that show if it is possible to determine if a curve is structural or non-structural or to assess flexibility of an adolescent idiopathic scoliosis (AIS) by recumbent images like a CT scan (CTS) instead of bending radiographs (BR). We investigated if the results of BR may be compared to those of CTS.

**Methods** We retrospectively analyzed prospectively collected data of patients with AIS in whom a selective spinal fusion was performed and in whom a CTS, BR, and full spine x-rays were made preoperatively. We measured the Cobb angles of the main and the minor curve in full spine x-ray, BR, and CTS.

**Results** After applying inclusion and exclusion criteria, 39 patients were included. We found a strong correlation ( $r=0.806$ ,  $p<0.01$ ) between the Cobb angle of the main curve in BR and the Cobb angle of the main curve in the CTS and between the Cobb angle of the minor curve in BR and the Cobb angle of the minor curve in the CTS ( $r=0.601$ ,  $p<0.01$ ). All patients with a minor curve of less than 25 degrees in the BR had a Cobb angle of less than 35 degrees in the CTS.

**Conclusion** Spinal curves showed a significant correlation between bending radiographs and recumbent images (CTS). In our group of patients, a Cobb angle of the minor curve of less than 35 degrees in the CTS indicated that this minor curve was non-structural.

**Keywords** Adolescent idiopathic scoliosis · Bending radiographs · Radiation protection · Selective spinal fusion

## Abbreviations

PPR	Push-prone radiographs
PIN	Pedicle screw insertion guided by navigation
CTS	Preoperative CT scan
FSR	Full spine x-ray in posterior–anterior view
ISE	Intervertebral space below the endvertebra of the main curve
FFI	Frist flexible intervertebral space below the main curve
AIS	Adolescent idiopathic scoliosis
LIV	Lowest instrumented vertebra
BR	Bending radiographs
R	Correlation
P	Level of significance

## Introduction

Adolescent idiopathic scoliosis (AIS) is a deformity of the spine with an incidence of 5% [1]. Depending on the degree of the deformity, assessed by the Cobb angle, conservative or operative therapy is recommended [2]. Patients with AIS who need an operative therapy may be treated with a selective spinal fusion. Important for the success of a selective spinal fusion is the discrimination of structural and non-structural curves of the total deformity according to the Lenke-Classification [3, 5] and to choose the appropriate lowest instrumented vertebra (LIV) [3, 4]. To classify a deformity according to the Lenke classification, bending radiographs (BR) of the spine are mandatory. Spinal curves, which can be reduced to less than 25° in a bending radiograph, are classified as “non-structural” [5]. Furthermore, BR allows assessing the possible potential for correction of the deformity by surgery [6, 7]. There are different types of bending radiographs: Push-prone radiographs (PPR) [8], fulcrum bending radiographs [6], supine side-bending radiographs [9], and radiographs with traction under General Anesthesia [10]. All types of BR lead to an additional

✉ Max Prost  
Max.prost@med.uni-duesseldorf.de

<sup>1</sup> Department of Orthopedic and Trauma Surgery, Medical Faculty and University Hospital Duesseldorf, Heinrich-Heine-University Duesseldorf, Düsseldorf, Germany

amount of exposure to radiation for the patient. Push-prone radiographs lead to an additional amount of radiation to the medical personal.

Other study groups [11, 12] showed that cumulative effective dose of standard radiographs, performed for diagnosis and follow-up of scoliosis correlates with incidence of breast cancer in scoliosis patients and with an increasing incidence for infertility. Therefore, it seems to be relevant to evaluate if the flexibility of the spine can be evaluated without BR. Some surgeons perform a preoperative CT scan (CTS), an MRI or an intraoperative recumbent radiograph if AIS is treated by surgery.

CTS are applied either for preoperative planning or as image acquisition for pedicle screw insertion guided by navigation (PIN).

Since these imaging techniques are performed recumbent, the difference between Cobb angles in standing or recumbent position could be evaluated to analyze flexibility.

To our knowledge, there is no data that shows if it is possible to determine if a curve is structural or non-structural by a recumbent imaging technique. If this would be possible BR might not be necessary anymore if, for other reasons, an MRI, a CTS or an intraoperative recumbent radiograph had been performed. This could lead to a reduction of the exposure to radiation for the patient and for the medical personnel.

We conducted this investigation to analyze if Cobb angles measured in CTS of the spine may render similar information on flexibility and type of curves as PPR.

## Patients and methods

We retrospectively analyzed prospectively collected data in a single center study. In our clinical documentation system, we identified consecutive patients in whom an operative treatment for AIS was performed from 05/2016 to 01/2020 by diagnostic code. We included patients who were treated by a selective spinal fusion guided by navigation and with image acquisition by preoperative CTS and who had a full spine x-ray in posterior–anterior view (FSR) and BR in the preoperative planning. In our institution PPR are performed as BR. BR were exclusively performed in patients who were treated by surgery, since these additional radiographs would lead to an additional amount of radiation without any change to the conservative therapeutic concept. We excluded patients with incomplete sets of radiological data. We recorded demographic data like sex, age, and date of menarche, as well as the Lenke-Classification of the included patients.

The radiographs were analyzed by the IDS 7-PACS®-System (Sectra, Linköping, Sweden). In all available radiographs (FSR, PPR, and the CTS) the Cobb angle of the main curve and of the upper and lower minor curve was measured.

Furthermore, we measured the segmental Cobb angle of the intervertebral space under the lowest vertebra of the main curve (ISE) and the angle of the first flexible intervertebral space below the main curve (FFI). Measurement of Cobb angle in the CTS is demonstrated in (Fig. 1). Measurement was performed in coronal reconstructions of the CT scan. End vertebrae were identified in the FSR. The angle between the superior endplate of the cranial end vertebra and the horizontal plane and the angle between the inferior endplate of the caudal end vertebra and the horizontal plane was measured. These two angles were added to obtain the Cobb angle of the according curve (Fig. 1).

## Identification and measurement of the ISE and the FFI

The lowest intervertebral space of the main curve was defined as the intervertebral space between the caudal end vertebra of the main curve and the cranial end vertebra of the caudal minor curve in the FSR. We measured the angle

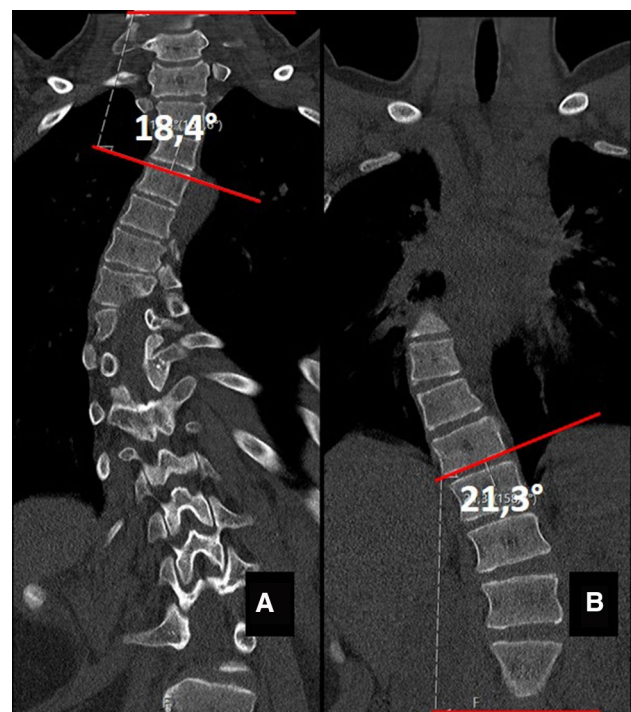


**Fig. 1** Measurement of Cobb Angle in a CTS. **a** Coronal reconstruction of a CT scan of the spine. The superior endplate of the cranial end vertebra of the according curve is depicted. End vertebra were identified in the FSR. The angle between the superior endplate of the cranial end vertebra and the horizontal plane was 18,4°. **b** Coronal reconstruction of a CT scan of the spine. The inferior endplate of the caudal end vertebra of the according curve is depicted. End vertebra were identified in the FSR. The angle between the inferior endplate of the caudal end vertebra and the horizontal plane was measured with 21,2 degrees. Summation of these two angles (18,4+21,2) gives us a Cobb angle of 39,6 degree for the complete thoracic deformity

between the inferior endplate of the cranial vertebra and the superior endplate of the caudal vertebra in the FSR, PPR, and the CTS.

The FFI below the main curve was defined as the intervertebral space caudal of the main curve of the deformity that opened to both sides in the PPR (Fig. 2). We measured the angle between the inferior endplate of the cranial vertebra of this intervertebral space and the superior endplate of the caudal vertebra in the FSR, PPR, and the CTS.

Statistical analysis was performed by SPSS® 25 (IBM, Armonk, USA). Descriptive data are given as mean and standard error of mean. We tested all continuous variables

for normal distribution by Kolmogorov–Smirnov tests. All variables showed normal distribution. Thus, we assessed correlation by Pearson's Correlation Index. Correlation ( $R$ ) and level of significance ( $p$ ) are reported. The differences of the measured Cobb angles showed significant outliers in the scatterplot and were therefore analyzed by Spearman's rank correlation coefficient.

For the analysis of the PPR, we always analyzed the angles of the PPR against the curve of interest: In curves with a right convexity, we analyzed the according PPR to the left and in curves with a left convexity, we analyzed the according PPR to the right.

This study was approved by the local ethics committee (Register number 2020–896) and was conducted according to the revised Declaration of Helsinki.

## Results

We identified 61 patients who were treated operatively for AIS in our institution between 05/2016 and 01/2020 and received a preoperative CT scan by diagnostic code. After application of the inclusion and exclusion criteria, we enrolled 39 patients to our investigation. 28 patients were female (72%), 11 patients were male (28%). The average age at the date the radiographs were performed was 18.23 (8.3) years. According to the Lenke classification 27 Patients had a type 1 curve, seven patients a type 5 curve, three patients type 2 and 2 patients a type 3 curve.

In Table 1, we present data of the Cobb angle of the main and of the minor curve in in the FSR, PPR and the CTS.

In a subgroup analysis of all patients with a minor curve of less than 40 degrees in the FSR (more than 40 degrees characterizes a structural curve) we analyzed the Cobb angles of the minor curve in the PPR and CTS. If the minor curve was less than 25 degrees in the PPR, it was less than 35 degrees in the CTS in 100% of these patients.

Tables 1, 2, 3 and 4 show values of Cobb angles of the FSR, PPR, and the CTS.

There was a strong correlation ( $r=0.746$ ,  $p<0.01$ ) between the Cobb angle of the main curve in FSR and the Cobb angle of the main curve in the CTS. Furthermore, there was a strong correlation ( $r=0.712$ ,  $p<0.01$ ) between the Cobb angle of the main curve in FSR and the Cobb angle

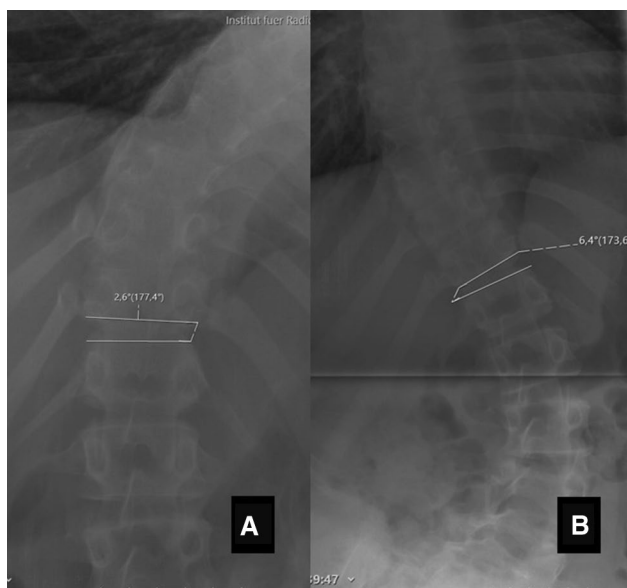


**Fig. 2** Identification of the FFI in the PPR. **a** PPR of the spine with Bending to the left. Zoom is on the caudal end of the main curve. End vertebra were identified in the FSR. Marked is the first intervertebral space below the main curve of the deformity that opens to the other side than the same intervertebral space in **b**. The angle between the inferior endplate of the cranial vertebra of this intervertebral space and the superior endplate of the caudal vertebra is measured. **b** PPR of the spine with Bending to the right. Zoom is on the caudal end of the main curve. End vertebra were identified in the FSR. Marked is the first intervertebral space below the main curve of the deformity that opens to the other side than the same intervertebral space in A. The angle between the inferior endplate of the cranial vertebra of this intervertebral space and the superior endplate of the caudal vertebra is measured

**Table 1** Cobb angle of the main and the minor curve in FSR, PPR, and the CTS

	Cobb angle of the main curve in FSR	Cobb angle of the minor curve in FSR	Cobb angle of the main curve in PPR	Cobb angle of the minor curve in PPR	Cobb angle of the main curve in CTS	Cobb angle of the minor curve in CTS
Mean	53,28	37,19	30,1053	17,3714	47,0000	34,7059
Standard deviation	9,736	12,269	11,99,051	14,00,648	11,51,497	12,13,692

**Table 2** Cobb angle of the ISE and FFI in FSR, PPR, and the CTS

	Cobb angle of the ISE in FSR	Cobb angle of the FFI in FSR	Cobb angle of the ISE in PPR	Cobb angle of the FFI in PPR	Cobb angle of the ISE in CTS	Cobb angle of the FFI in CTS
Mean	428	460	−23,865	−35,737	33,795	36,868
Standard deviation	2578	2812	462,380	293,706	332,718	370,085

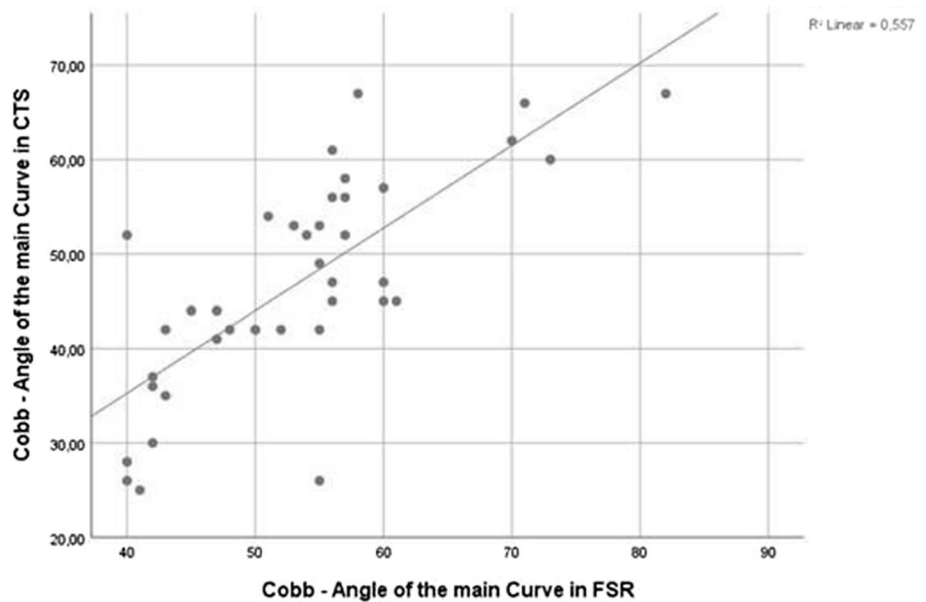
**Table 3** Difference of the Cobb angle of the main curve and minor curve in FSR and PPR and in the in FSR and the CTS

	Difference in Cobb angle of the main curve in FSR and PPR	Difference in Cobb angle of the minor curve in FSR and PPR	Difference in Cobb angle of the main curve in FSR and CTS	Difference in Cobb angle of the minor curve in FSR and CTS
Mean	240,256	211,974	64,211	35,441
Standard deviation	893,393	1,058,399	776,211	778,924

**Table 4** Difference Cobb angle of the ISE and FFI in FSR and PPR and in the FSR and the CTS

	Difference in Cobb angle of the ISE in FSR and PPR	Difference in Cobb angle of the FFI in FSR and PPR	Difference in Cobb angle of the ISE in FSR and CTS	Difference in Cobb angle of the FFI in FSR and CTS
Mean	56,703	81,737	9000	9132
Standard deviation	395,832	337,308	257,294	277,374

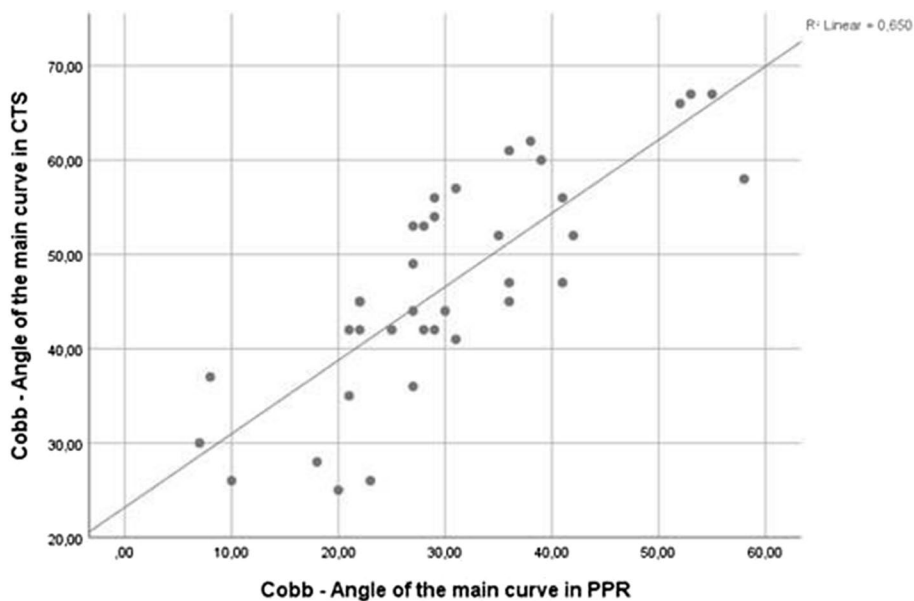
**Fig. 3** Correlation between the Cobb angle of the main curve in CTS and FSR. In this scatterplot, the correlation between the Cobb angle of the main curve in CTS and FSR is presented. On the x-axis, the Cobb angle (°) of the of the main curve in the FSR is shown. On the y-axis, the correlated Cobb angle (°) of the of the main curve in the CTS is shown



of the main curve in the PPR. We also found a strong correlation ( $r=0.806, p < 0.01$ ) between the Cobb angle of the main curve in PPR and the Cobb angle of the main curve in the CTS. See also Figs. 3 and 4

Furthermore, we found significant correlations between the minor curves in the different types of radiographs. There was a strong correlation ( $r=0.671, p < 0.01$ ) between the Cobb angle of the minor curve in FSR and the Cobb angle of the minor curve in the PPR. There also was a strong

**Fig. 4** Correlation between the Cobb angle of the main curve in CTS and PPR. In this scatterplot, the correlation between the Cobb angle of the main curve in CTS and PPR is presented. On the x-axis, the Cobb angle (°) of the of the main curve in the PPR is shown. On the y-axis, the correlated Cobb angle (°) of the of the main curve in the CTS is shown



correlation ( $r=0.802$ ,  $p<0.01$ ) between the Cobb angle of the minor curve in FSR and the Cobb angle of the minor curve in the CTS. We also found a strong correlation ( $r=0.601$ ,  $p<0.01$ ) between the Cobb angle of the minor curve in PPR and the Cobb angle of the minor curve in the CTS (Figs. 5 and 6).

There was a strong correlation ( $r=0.675$ ,  $p<0.01$ ) between the Cobb angle in the ISE in the FSR and in the PPR. There also was a strong correlation ( $r=0.647$ ,  $p<0.01$ ) between the Cobb angle in the ISE in the FSR and in the CTS. There was a significant correlation ( $r=0.681$ ,  $p<0.01$ ) between the Cobb angle in the ISE in the PPR radiographs and the CTS.

There was no strong correlation ( $r=0.312$ ,  $p>0.05$ ) between the Cobb angle in the FFI in the FSR and in the PPR. But there was a strong correlation ( $r=0.668$ ,  $p<0.01$ ) between the Cobb angle in the ISE in the FSR and in the CTS. There was a strong correlation ( $r=0.484$ ,  $p<0.01$ ) between the Cobb angle in the FFI in the PPR radiographs and the CTS.

The difference between the Cobb angle of the main curve in the FSR and in the PPR shows a strong correlation ( $r=0.424$ ,  $p<0.01$ ) to the difference between the Cobb angle of the main curve in the FSR and the Cobb angle of the main curve in the CTS. The difference between the Cobb angle of the minor curve in the FSR and in the PPR shows

**Fig. 5** Correlation between the Cobb angle of the minor curve in FSR and CTS. In this scatterplot, the correlation between the Cobb angle of the minor curve in FSR and CTS is presented. On the x-axis, the Cobb angle (°) of the of the minor curve in the FSR is shown. On the y-axis, the correlated Cobb angle (°) of the of the minor curve in the CTS is shown

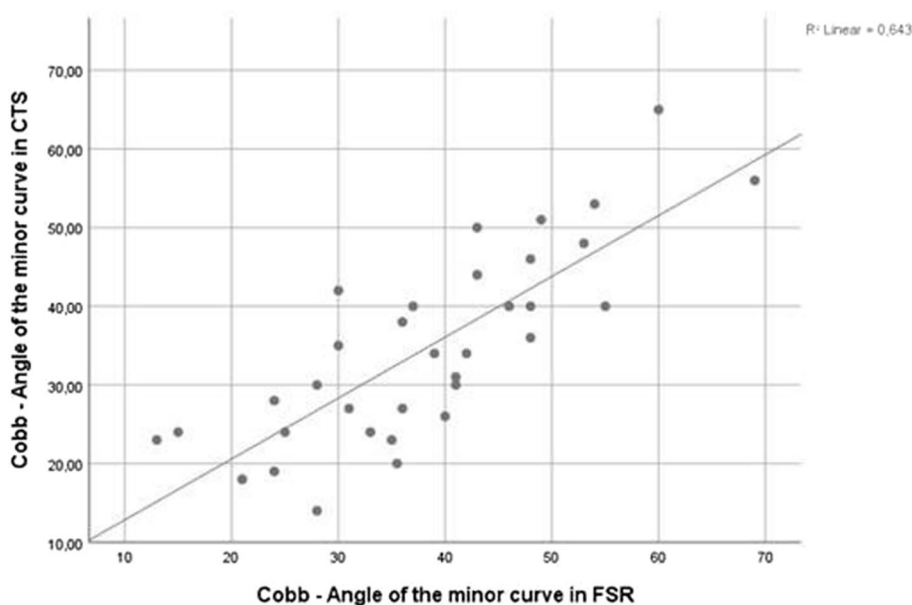
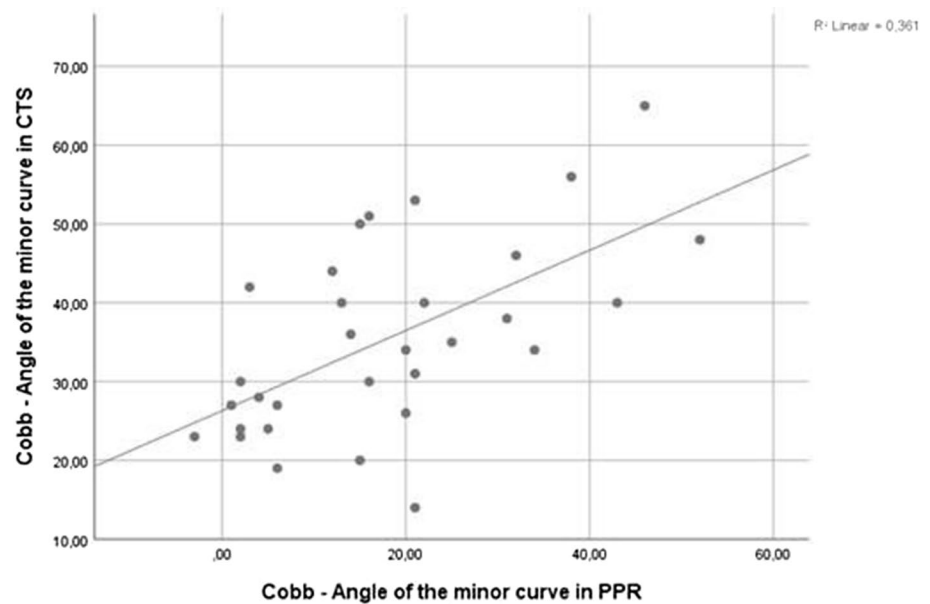




**Fig. 6** Correlation between the Cobb angle of the minor curve in PPR and CTS. In this scatter-plot, the correlation between the Cobb angle of the minor curve in PPR and CTS is presented. On the x-axis, the Cobb angle (°) of the of the minor curve in the PPR is shown. On the y-axis, the correlated Cobb angle (°) of the of the minor curve in the CTS is shown



a strong correlation ( $r=0.305$ ,  $p<0.05$ ) to the difference between the Cobb angle of the minor curve in the FSR and the Cobb angle of the minor curve in the CTS. There was a strong correlation ( $r=0.388$ ,  $p<0.01$ ) between the difference of the Cobb angle of the FFI in the FSR and in the PPR and the difference of the Cobb angle of the FFI in the FSR and in the CTS.

## Discussion

In this study, we analyzed the FSR, PPR, and the CTS from 39 patients who were treated by surgery for AIS. We analyzed if there are significant correlations in the measured Cobb angles of the main and the minor curves in the FSR, the PPR and the CTS and if there are correlations in the Cobb angles of the ISE and the FFI in the different imaging techniques. We found significant correlation ( $p<0.01$ ) for all analyzed Cobb angles between BR and CTS.

Brink et al. reported a significant correlation of the morphology of the scoliotic spine in all three planes between standard upright X-ray, MRI, and CT scan [13]. Keenan et al. showed 2014 that there is a statistically significant relationship between the Cobb angle in supine and upright position for the major curve [14]. However, minor curves were not analyzed, especially not regarding to the flexibility. There is presently no data that compares the assessment of flexibility of the minor curve in BR versus CT scans. We therefore conducted this study to analyze if classification of minor curves according to the Lenke classification [3] may be possible by a recumbent CT scan.

In our group of patients, we were able to show, that Cobb angles of the main and the minor curves in the CTS show a significant correlation to Cobb angles in FSR and PPR.

We found a significant correlation of the difference of the Cobb angles of the main and minor curves between FSR and CTS with the difference of the Cobb angles of the main and minor curves between FSR and PPR. This indicates that Cobb angles of the main and the minor curves in CTS may provide similar information as a PPB.

Furthermore, our data show that it is possible to determine if a minor curve is structural or non-structural according to the measured Cobb angle in the CTS. We looked at every patient with a Cobb angle of the minor curve of less than 40 degrees in the FSR and a Cobb angle of the minor curve less than 25 degrees in the PPB. These curves are, according to the Lenke classification, non-structural and do not have to be included in the selective spinal fusion [3]. In this group of patients, the Cobb angle of the minor curve in the CTS was always less than 35 degrees. According to this data, in our group of patients a Cobb angle of  $<35^\circ$  determined a non-structural curve. This indicates that PPR's are not necessary anymore to determine if a curve is structural or non-structural, if for any reason a preoperative CT scan has been performed. This may lead to a reduction of dose of radiation for the patients and for the medical personal.

Furthermore, we saw that there are significant correlations between the Cobb angles of the ISE and the FFI in the analyzed radiographs. However, statistical power was rather low especially in the correlations between the PPR and the CTS. Thus, we presently cannot apply the CTS as a tool to analyze the flexibility of the ISE and the FFI.

A limitation of our investigation is that we performed a retrospective data analysis. Furthermore, we only performed

and analyzed the correlation between the PPR and the CTS and did not investigate the impact of other types of BR. However, former analyses showed that PPR are the most appropriate type of BR to determine the effects of a correction of the main curve on the curves above and below the level of fusion by better predicting the translational correction of the lowest instrumented vertebra and the rotation of the lowest instrumented vertebra than other types of BR [15]. Other investigations detailed characteristics of the different types of BR. Fulcrum bendings are the most appropriate images to assess the maximal preoperative coronal flexibility in main thoracic curves, side-bending radiographs are the most appropriate images to assess the maximal preoperative coronal flexibility in main thoracolumbar or lumbar curves [16]. Radiographs with traction under General Anesthesia lead to a higher degree of correction of severe curves ( $> 60^\circ$ ). However, it has also been shown that selection of lowest instrumented vertebra based on traction radiographs leads to an increased frequency of decompensation of the non-instrumented lower spinal segments [10, 17]. The available data show that none of the common types of BR is superior to the others [6, 8, 10, 15–17].

The primary objective of this investigation was to analyze if recumbent images could “replace” BR in the diagnostic algorithm of AIS. Since some of our patients were operated by navigation based on a preoperative CTS, we used these CTS images as recumbent imaging technique in this investigation and found that CTS may be applied to classify scoliotic minor curves as structural or non-structural. We presently avoid performing any more pedicle screw insertions guided by navigation (PIN) with preoperative CTS in AIS patients because of the higher exposure to radiation of the patients, but applying navigation by an intraoperative 3D scan [18]. For the same reason, we now aspire to apply different recumbent imaging techniques, i.e., MRI or intraoperative images, as “replacement” for BR. Thus, future investigations should focus on whether other recumbent imaging techniques are as effective as CT scans to classify curve flexibility in scoliosis patients.

## Conclusion

Cobb angles of push-prone bending radiographs show a significant correlation with Cobb angles in CT scans. In our group of patients, a Cobb angle of a minor curve in a CT scan of less than  $35^\circ$  determined a non-structural curve in 100% of all cases.

**Author's contributions** MP involved in conception and design, administrative support, collection and assembly of data, provision of study materials or patients, data analysis and interpretation, manuscript

writing, and final approval of manuscript. JW participated in administrative support, provision of study materials or patients, manuscript writing, and final approval of manuscript. MRK involved in conception and design, administrative support, provision of study materials or patients, data analysis and interpretation, manuscript writing, and final approval of manuscript.

**Funding** Open Access funding enabled and organized by Projekt DEAL. No benefits in any form have been received or will be received from a commercial party related directly or indirectly to the subject of this article.

**Data availability** The datasets generated during and / or analyzed during the current study are not publicly available due data protection but are available from the corresponding author on reasonable request.

## Declarations

**Conflicts of interest** MRK reports personal fees from Globus Medical, outside the submitted work. The other authors declare no conflict of interest relevant to this work.

**Ethics approval** This study was approved by the local ethics committee (registry number 2020–896) and was conducted according to the revised declaration of Helsinki.

**Open Access** This article is licensed under a Creative Commons Attribution 4.0 International License, which permits use, sharing, adaptation, distribution and reproduction in any medium or format, as long as you give appropriate credit to the original author(s) and the source, provide a link to the Creative Commons licence, and indicate if changes were made. The images or other third party material in this article are included in the article's Creative Commons licence, unless indicated otherwise in a credit line to the material. If material is not included in the article's Creative Commons licence and your intended use is not permitted by statutory regulation or exceeds the permitted use, you will need to obtain permission directly from the copyright holder. To view a copy of this licence, visit <http://creativecommons.org/licenses/by/4.0/>.

## References

1. Konieczny MR, Senyurt H, Krauspe R (2013) Epidemiology of adolescent idiopathic scoliosis. *J Child Orthop* 7(1):3–9. <https://doi.org/10.1007/s11832-012-0457-4>
2. Trobisch P, Suess O, Schwab F (2010) Idiopathic scoliosis. *deutsches ärzteblatt. International* 107(49):875
3. Lenke LG, Betz RR, Haher TR, Lapp MA, Merola AA, Harms J, Shufflebarger HL (2001) Multisurgeon assessment of surgical decision-making in adolescent idiopathic scoliosis: curve classification, operative approach, and fusion levels. *Spine* 26(21):2347–2353. <https://doi.org/10.1097/00007632-200111010-00011>
4. King HA, Moe JH, Bradford DS, Winter RB (1983) The selection of fusion levels in thoracic idiopathic scoliosis. *J Bone Joint Surg Am* 65(9):1302–1313
5. Lenke LG, Betz RR, Harms J, Bridwell KH, Clements DH, Lowe TG, Blanke K (2001) Adolescent idiopathic scoliosis: a new classification to determine extent of spinal arthrodesis. *J Bone Joint Surg Am* 83(8):1169–1181 (PMID: 11507125)
6. Cheung KMC, Luk KDK (1997) Prediction of correction of scoliosis with use of the fulcrum bending radiograph. *JBJS* 79(8):1144–1150

7. Kleinman RG, Csongradi JJ, Rinsky LA, Bleck EE (1982) The radiographic assessment of spinal flexibility in scoliosis: a study of the efficacy of the prone push film. *Clin Orthop Relat Res.* (162):47–53. PMID: 7067232
8. Rodrigues LM, Ueno FH, Gotfryd AO, Mattar T, Fujiki EN, Milani C (2014) Comparison between different radiographic methods for evaluating the flexibility of scoliosis curves. *Acta ortopédica brasileira* 22(2):78–81. <https://doi.org/10.1590/1413-78522014220200844>
9. Aronsson DD, Stokes IA, Ronchetti PJ, Richards BS (1996) Surgical correction of vertebral axial rotation in adolescent idiopathic scoliosis: prediction by lateral bending films. *J Spinal Disord* 9(3):214–219
10. Vaughan JJ, Winter RB, Lonstein JE (1996) Comparison of the use of supine bending and traction radiographs in the selection of the fusion area in adolescent idiopathic scoliosis. *Spine* 21(21):2469–2473. <https://doi.org/10.1097/00007632-199611010-00012>
11. Doody MM, Lonstein JE, Stovall M, Hacker DG, Luckyanov N, Land CE (2000) Breast cancer mortality after diagnostic radiography: findings from the U. S. Scoliosis cohort study. *Spine* 25(16):2052–2063. <https://doi.org/10.1097/00007632-200008150-00009>
12. Simony A, Christensen SB, Jensen KE, Carreon LY, Andersen MO (2015) Incidence of cancer and infertility in patients treated for adolescent idiopathic scoliosis 25 years prior. *Eur Spine J.* <https://doi.org/10.1007/s00586-015-4130-8>
13. Brink RC, Colo D, Schlösser T, Vincken KL, van Stralen M, Hui S, Shi L, Chu W, Cheng J, Castelein RM (2017) Upright, prone, and supine spinal morphology and alignment in adolescent idiopathic scoliosis. *Scol. Spin. Dis.* 12:6. <https://doi.org/10.1186/s13013-017-0111-5>
14. Keenan BE, Izatt MT, Askin GN, Labrom RD, Pearcy MJ, Adam CJ (2014) Supine to standing Cobb angle change in idiopathic scoliosis: the effect of endplate pre-selection. *Scoliosis* 9:16. <https://doi.org/10.1186/1748-7161-9-16>
15. Vedantam R, Lenke LG, Bridwell KH, Linville DL (2000) Comparison of push-prone and lateral-bending radiographs for predicting postoperative coronal alignment in thoracolumbar and lumbar scoliotic curves. *Spine* 25(1):76–81. <https://doi.org/10.1097/00007632-200001010-00014>
16. Klepps SJ, Lenke LG, Bridwell KH, Bassett GS, Whorton J (2001) Prospective comparison of flexibility radiographs in adolescent idiopathic scoliosis. *Spine* 26(5):E74–E79. <https://doi.org/10.1097/00007632-200103010-00002>
17. Pruijs JE, Hageman MA, Keessen W, van der Meer R, van Wieringen JC (1994) Variation in Cobb angle measurements in scoliosis. *Skeletal Radiol* 23(7):517–520. <https://doi.org/10.1007/BF00223081>
18. Konieczny MR, Boos J, Steuwe A, Schleich C, Prost M, Krauspe R (2020) Effective dose of radiation per screw in surgery of adolescent idiopathic scoliosis: matched pair analysis of 293 pedicle screws inserted using three different techniques. *J Child Orthop* 14(6):554–561. <https://doi.org/10.1302/1863-2548.14.200148>

**Publisher's Note** Springer Nature remains neutral with regard to jurisdictional claims in published maps and institutional affiliations.